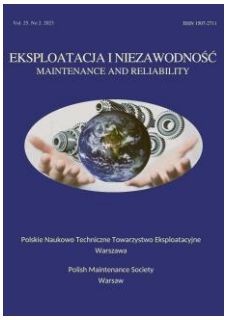

Eksploatacja i Niezawodnosc – Maintenance and Reliability
Volume 28 (2026), Issue 4
journal homepage: http://www.ein.org.pl

Article citation info:
Knypiński Ł, Kasprzak K, Joddumanhanthi V, Adaptation of the whale optimization algorithm to multi-objective and constrained optimization of the brushless DC motor, Eksploatacja i Niezawodnosc – Maintenance and Reliability 2026: 28(4) http://doi.org/10.17531/ein/220513

Adaptation of the whale optimization algorithm to multi-objective and constrained optimization of the brushless DC motor

Indexed by: Web of Science Group

Łukasz Knypiński[a,*], Kacper Kasprzak[a], Vijaychandra Joddumahanthi[b]

[a] Instiitute of Electrical Engineering and Electronic, Poznan University of Technology, Poland
[b] Department of Electrical & Electronics Engineering, Lendi Institute of Engineering and Technology, India

Highlights

- Adaptation of the whale algorithm to multi-objective and constrained optimization.
- Optimal design of the brushless DC motor to the electric vehicle.
- The performance reliability of two heuristic algorithm was compared, i.e. (a) WOA, (b) PSO.

Abstract

This paper presents the algorithm and computer script for the multi-objective and constrained optimization of the brushless DC motors for the propulsion of the electric vehicles. The optimization procedure was developed on the basis of the whale optimization algorithm and tested using the selected benchmark function. The universal analytical model of the brushless DC motor (BLDC) was developed. The designed motor is described by four design variables. The methodology of the two-stage adaptation of the whale optimization algorithm to multi-objective and constrained optimization of the electromagnetic devices are proposed. The developed adaptation improved the efficiency and reliability of the optimization procedure. The multi-objective compromise function contains two functional parameters of the designed motor: efficiency and total materials mass. In the case of the constrained optimization problem, the total mass of the designed motor was minimized and efficiency was maximized, whereas winding temperature was taken into account as a constraints. Selected results of the optimization calculation were presented and discussed.

Keywords
algorithm adaptation, multi-objective optimization, constrained optimization, whale optimization algorithm, brushless DC motor

1. Introduction

Optimization algorithms are more and more commonly applied in electrical machines optimal design [1,2], just like in other fields requiring devices and systems with strictly and precisely defined properties [3]. If optimization algorithms do not determine an optimal solution, then they certainly indicate what affects the parameters of the designed device or system significantly [4].

Nowadays, many papers are devoted to the application of various metaheuristic optimization algorithms in the optimal design of electromagnetic devices [5]. Those papers are divided into two main groups: (a) application to optimization algorithms to improve various parameters of designed devices [6,7], and (b) development of new, more efficient, and reliable optimization algorithms [8]. The previous decade has brought enormous development of metaheuristic optimization algorithms that can successfully and powerfully support the design process of the electromagnetic devices [9].

The large number of available metaheuristic optimization algorithms and the diversity of their mathematical models and algorithm properties [10] allow that, before starting to solve the optimization problem, the researcher must select an appropriate algorithm [11]. After selecting a proper optimization algorithm,

(*) Corresponding author.
E-mail addresses: Ł. Knypiński (ORCID: 0000-0001-5741-9548) lukasz.knypinski@put.poznan.pl, K. Kasprzak (ORCID: 0009-0001-5641-6449) kacper.kasprzak@student.put.poznan.pl, V. Joddumahanthi (ORCID: 0000-0001-9741-9358) vijaychandrajvc@gmail.com

it is necessary to select proper values of the characteristic coefficients of the optimization algorithm. The correct selection of the characteristic coefficients is named adaptation. Proper adaptation process is very important and ensures balance between exploration and exploitation, which guarantee the efficiency and convergence of the optimization algorithm, and reliability in escapes from local optima points [12].

In the articles devoted on the optimization of brushless DC motors published in the last three years, analytical models and lumped parameter models are mostly used for optimization, and the finite element models are rarely used. In [13], an analytical model was used to optimize a BLDC motor. A simplified lumped parameter model was applied in [14], and the results of optimization calculations were verified after building a prototype of the BLDC motor. Articles [15,16] present an application of a simplified BLDC motor model to execute optimization the control system. 3D models are most often used to optimize complex motor structures that cannot be considered in 2D models [17].

The whale optimization algorithm (WOA) is an interesting approach among nature-inspired optimization algorithms. The optimization process is modelled on the whale hunting process [18]. This algorithm includes different mechanism such as: enveloping the prey phenomena, hunting by bubble strategy, and random search [19]. WOA includes the spiral motion of the hunting whales. Spiral searching of all individuals allows for finding a better solution, located around the best-adapted whale. The algorithm is resistant to getting stuck at local extremum points via a random search mechanism. The algorithm is also characterized by good convergence and reliability at searching global solution [20]. The whale optimization algorithm has often been used to solve various engineering problems [21,22]. The actual literature lacks approaches to adapting the WOA algorithm for multi-objective optimization and constraint optimization in the design of electromagnetic devices. The paper presents the approach of two-stage adaptation of the WOA algorithm and its impact on the efficiency and reliability of optimization algorithm.

The aim of this work is to develop an optimization procedure using WOA and an adaptation of this algorithm to multi-objective and constrained optimization of the BLDC motor intended to the propulsion of electric vehicles.

The main contributions of this paper are as follows:

- An adaptation of the metaheuristic WOA to multi-objective optimization of electromagnetic devices, especially permanent magnet motors, was proposed. The non-linear changes [23] of the characteristic coefficient optimization algorithm to obtain faster convergence.
- The approach with a smooth increase of the penalty coefficient is proposed. In the developed method, the penalty coefficient is changed in each iteration of the optimization algorithm. The use of smooth changes in the coefficient increases the performance and reliability of the optimization algorithm.
- An adaptation of the WOA algorithm was developed to take into account constraints in the optimal design of electromagnetic devices. This adaptation involves nonlinearly increasing the penalty coefficient in each iteration of the algorithm. Nonlinear changes of the penalty coefficient improve the performance of the optimization algorithm.
- A methodology for two-stage adaptation of the WOA optimization algorithm is presented [24]. The first stage involves adapting the characteristic coefficients of the optimization algorithm. The second stage involves adapting the way of changes penalty coefficient.

The social interactions in whale pod and mathematical model of optimization algorithm are presented in section 2. The correctness test of the optimization procedure using selected benmarch function is presented in section 3. Mathematical model of optimized BLDC motors is described in Section 4. Next the result of multi-objective and constrained optimization are presented in Section 5. The section 6 presents the finite method analysis and comparison the optimal results obtained for analytical model The summarizing conclusions are discussed in section 7.

2. Whale optimization algorithm

Whale optimization algorithm was proposed by S. Mirjalili and A. Lewis in 2016 [25]. The algorithm is based on the hunting behaviour of some whale species. Whales are one of the most intelligent animals in World [26], hence the idea of using the hunting mechanism to develop an optimization algorithm. The hunting is a very complex process [27]. Papers [28,29] describe

two types of hunting behaviour which will affect the whale optimization algorithm. WOA is included in the group of swarm intelligence methods [30].

The whale optimization algorithm involves determining the positions of all individuals in the pod using the position of the best-adapted or random whale. In the first iteration (initiation) positions of all whales are generated randomly. In the next stage hunting method is selected. The probability of choosing a specific hunting method is equal. To do this, random p number is generated from range [0,1]. In the next step positions of all whales change according to equations [31]. If p<0.5 then the siege mechanism is used. In this mechanism, the first operation that needs to be done is to calculate the values of characteristic parameters, that will change at each iteration:

$$A_i^k = 2 \cdot a \cdot r_1 - a, C_i^k = 2 \cdot r_2 \quad (1)$$

where: k is the iteration number, r_1, r_2 are the randomly generated numbers from range $[0,1]$, a non-linear decrease coefficient from 2 to 0 with the increasing number of iteration. In the next stage position of whales are calculated:

$$X_i^{k+1} = X_i^* - A_i^k \cdot \left| C_i^k \cdot X_i^* - X_i^k \right| \quad (2)$$

where: X_i^* is the possible position of prey and it depends on the value of $|A|$. If $|A| < 1$ then $X_i^* = X_i^{best}$, where X_i^{best} is the position of best-adapted whale in pod. Otherwise ($|A| \geq 1$) $X_i^* = X_i^{rand}$, where X_i^{rand} is the position of the randomly selected whale.

As mentioned above, the hunting mechanism is chosen based on the value of the random number p. The spiral model is used when p≥0.5. In that case, calculating D' is necessary:

$$D_i'^k = \left| X_i^{best} - X_i^k \right| \quad (3)$$

Finally, position of all whales is calculated using formula:

$$X_{i+1}^k = D_i'^k \cdot e^{bl} \cdot cos(2\pi l) + X_i^{best} \quad (4)$$

where: b is the constant number, l is the generated randomly from range [-1,1].

The flowchart of the elaborated optimization procedure is presented on Figure 1.

3. Correctness test of the optimization procedure

The optimization algorithm and procedure based on WOA were developed in a Python programming environment. Then the correctness of the optimization procedure was checked using the drop-wave benchmark function.

The drop-wave benchmark function is described by formula:

$$f(x_1, x_2) = -\frac{1+\cos\left(12\sqrt{x_1^2+x_2^2}\right)}{0{,}5(x_1^2+x_2^2)+2} \quad (5)$$

where: x_1 is included the range (–2.0, 2.0), x_2 is included in the range (–2.0, 2.0).

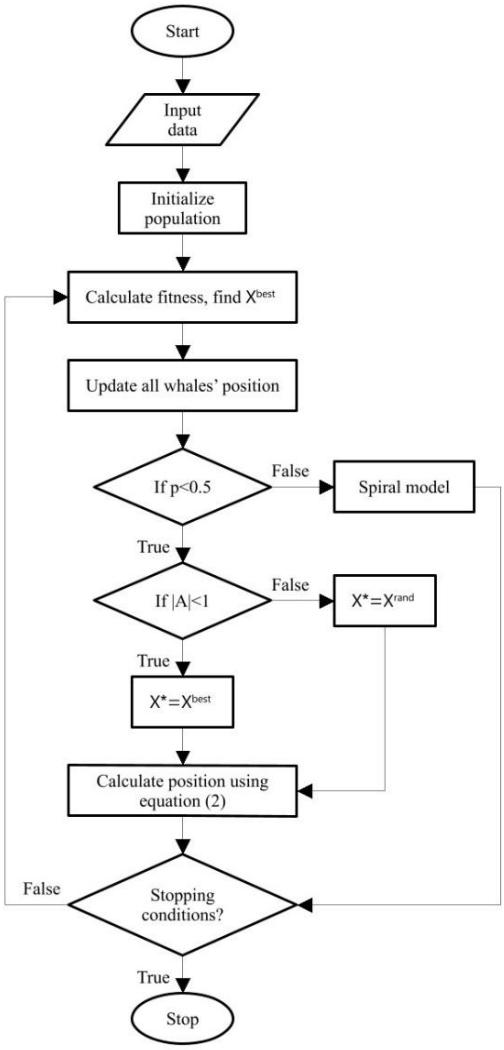

Figure 1. The block diagram of the developed WOA algorithm.

The drop-wave function is a multimodal function with one global minimum and multiple local optima. Global minimum is attained for $x_1 = 0$ and $x_2 = 0$ and it is equal to $f(0,0) = -1$ [32]. Figure 2 presents a 3D plot of drop-wave function when $x_1, x_2 \in [-1,1]$.

During testing computation, a population of 50 whales and a maximal number of iterations equal to 40 were adapted. The optimization software was run 25 times for random initial populations. The a coefficient are non-linearly decreased in successive iterations of optimization process and b coefficient equal 1.

For a series of 25 starts of the optimization procedure, the statistical analysis was done. The best, worst results from the

series, average (AV) objective function and standard deviation (SD) were determined.

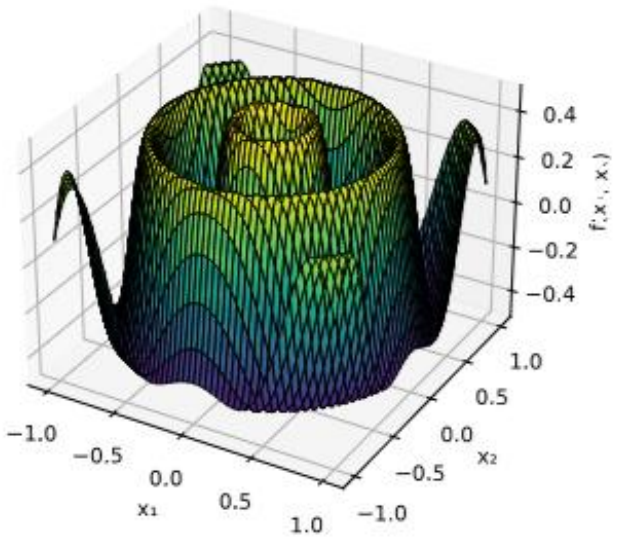

Figure 2. 3D visualization of drop-wave function.

Next, the series of optimization computations for the drop-wave function using the particle swarm optimization (PSO) algorithm were executed. The PSO algorithm was chosen as the reference method because it is often applied as a comparison method for new optimization algorithms [33,34]. The PSO algorithm ensures high efficiency, good convergence and reliability in finding the global extremum point. The values of characteristic coefficients of the PSO are adopted: w_1=0.2, c_1=0.35, c_2=0.45.

Table 1 presents the statistical analysis results for a series of 25 runs of the optimization procedures for both optimization algorithms.

Table 1. Statistical analysis for drop-wave function for both algorithms.

Algorithm		Best	Worst	AV	SD
WOA	$f(x_1, x_2)$	-1.00000000	-0.93624	-0.993624	0.019160
	x_1	0.000000017	0.01873	0.01874	0.059121
	x_2	0.000000017	-0.48545	-0.04861	-0.04862
PSO	$f(x_1, x_2)$	-1.000000000	-0.93624	-0.98724	0.026881
	x_1	-0.000000037	-0.018696	-0.02643	0.152623
	x_2	0.000000001	-0.48545	-0.07863	0.171318

Based on Table 1, it can conclude that a similar objective function value for the best result was obtained for both tested algorithms. And, interestingly, both algorithms "get stuck" at the same local extremum point, they obtain the same values of the objective function and coordinates x_1 and x_2. The WOA algorithm obtained a lower value of the average objective function value from the analyzed series of optimization calculations. The most important parameter that allows to the rating of the quality of the optimization algorithm is the standard deviation. The SD determines how repeatable the results of the optimization procedure are and what is the probability of determining the global optimum with a single run of the algorithm. The WAO algorithm allows for obtaining better SD than PSO. The results confirmed that whale optimization algorithm is an interesting algorithm in the group of nature-inspired optimization algorithms.

The authors did not analyzed of the number of call functions in this paper, because for both compared optimization algorithms, the number of call functions is the same. An analysis of the total optimization time will be discussed for the constrained optimization problem.

Next, the convergence curves were compared for the processes ending with the best result. Figure 3 compares the convergence curve for WAO and PSO algorithms.

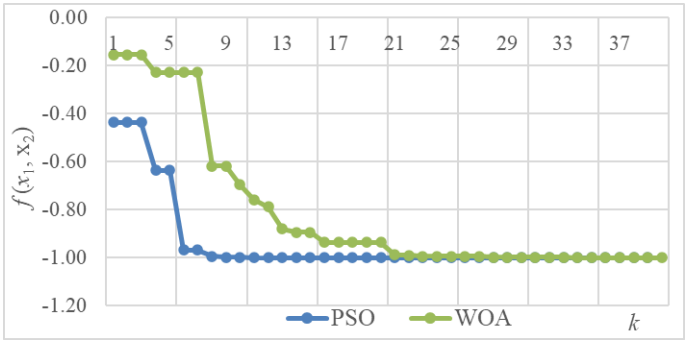

Figure 3. Comparison the convergence curves for WOA and PSO algorithms.

Based on the results presented in Fig. 3, it can be concluded that classical PSO is characterized by faster convergence than WOA. The faster convergence is due to the strong forces that concentrate the particles around the swarm leader (swarming behaviors).

4. Mathematical model of outer-rotor brushless DC motor

The mathematical model of the optimized BLDC motor was developed on non-linear equations describing phenomena occurring in electromagnetic devices, as well as in rotary electrical machines. The structure of the motor with marked structural dimensions is presented in Figure 4.

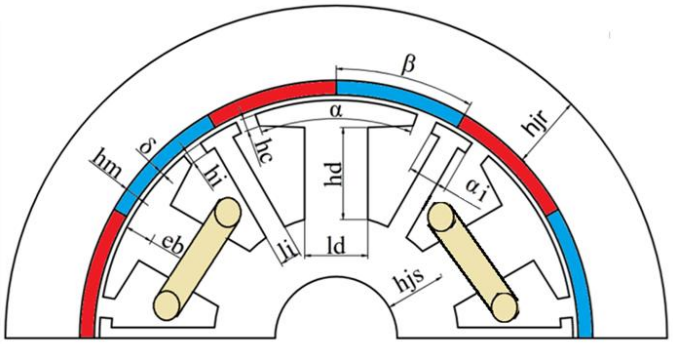

Figure 4. BLDC motor structure.

During developing the model the phenomena describing the electromagnetic field, thermal field, and equation describing motion are taken into account [35,36]. Based on the electromechanical conversion law, the mechanical power produced by the BLDC motor can be determined [35]:

$$P_m(t) = T(t)\omega(t) = e_A(t)i_A(t) + e_B(t)i_B(t) + e_C(t)i_C(t) \quad (6)$$

where: T is the value of electromagnetic torque, ω is the angular velocity, i_A, i_B, and i_C are the phase currents, e_A, e_B, and e_C are the back-electromotive forces induced in the stator winding.

In steady-state operation equation (6) has form:

$$T\omega = 2EI \quad (7)$$

The back-electromotive force (back-EMF) induced in the stator winding in the BLDC motor is calculated:

$$E = \frac{n}{4} B_\delta D_o L_m \omega \quad (8)$$

in which: n is the number turns in single phase, B_δ is the maximum value of magnetic flux density in the air gap, D_O is the outer rotor diameter, L_m is the stack length.

Next, based on the assumed functional parameters and vector of design variables, all dimensions of the designed BLDC motor are determined [36]. Taking into consideration the shape of the BLDC structure and the adopted material properties for the ferromagnetic core, copper and permanent magnets, the total mass of the designed motor is determined:

$$m_t = m_{pm} + m_{cu} + m_y + m_{rsr} \quad (9)$$

where: m_{pm} is the mass of permanent magnets, m_{cu} is the mass of the copper used to construct the winding, m_y is the mass stator and rotor yokes, m_{rsr} is the mass of the stator teeth.

The losses in an elaborated model are calculated as copper and iron losses. The cooper losses are determined:

$$P_{cu} = 2I^2 R_p \quad (10)$$

where: R_p is the phase resistance, $R_p = \rho_{cu}(1 + \alpha_{cu}\vartheta_w)\frac{n}{2} L_w \frac{J_w}{I}$, ρ_{cu} is the copper resistivity, α_{cu} is the cooper thermal factors, ϑ_w is the steady-state winding temperature, n is the number turns in one phase, L_w is the average length of winding wire.

Losses in the ferromagnetic core are determined as follows:

$$P_{fe} = q_t \left(\frac{f}{f_c}\right)\left[m_{sy}\left(\frac{B_{sy}}{B_c}\right)^2 + m_{ts}\left(\frac{B_s}{B_t}\right)^2\right] \quad (11)$$

where: q_t is the catalog core losses for frequency f_c and magnetic flux density B_c equal 50 Hz and 1.5 T respectively, m_{sy} is the stator yoke mass, B_{sy} is the value of magnetic flux density in stator yoke, m_{ts} is the stator teeth mass, B_s is the average magnetic flux density in stator teeth, $f = \frac{p\omega}{2\pi}$, p is the number of pole pairs.

The efficiency of the BLDC motor describes the following equation:

$$\eta = \frac{T\omega - P_{mech}}{T\omega + P_{cu} + P_{fe}} \quad (12)$$

in which P_{mech} is the mechanical losses.

In the proposed approach thermal model of the phenomena, it was assumed that the stator winding temperature is equal to the temperature of the permanent magnets $\vartheta_w = \vartheta_{pm}$, in steady-state operation. The elaborated thermal model assumes that the heat is abandoned to the environment through the outer surface of the BLDC motor. The heat abandoned surface is determined by:

$$S_\vartheta = \frac{\pi}{2} D_{so}^2 + \pi L_t D_{so} \quad (13)$$

where: D_{so} is the outer stator diameter, L_t is the total axial length of the motor.

Finally, the winding and permanent magnet temperature in steady-state operation is calculated:

$$\vartheta_w = \vartheta_{pm} = \vartheta_a + \frac{P_{cu} + P_{fe} + P_{mech}}{h S_\vartheta} \quad (14)$$

where: ϑ_a is the ambient temperature, h is the air convection coefficient.

5. Results of optimization calculation

5.1. Multi-objective optimization

The designed outer-rotor BLDC motor is intended to be a drive motor for electric bikes. Based on the results of research concerning on the design of motors for bicycle propulsion, the following parameters of the motor have been assumed: rated value of torque T_N=10 Nm, rated supply voltage U_N=36 V, rated

velocity n_N=280 rpm, and no-load velocity n_{max}=420 rpm [37,38].

The aim of the optimization is determining the vector of design variables of the BLDC motor ensuring the maximum value of the multi-objective function or modified objective function. The objective function includes two important functional parameters: efficiency and total material mass of the motor. The outer-rotor BLDC motor is described by four design variables: D_O – is the outer rotor diameter, B_δ – is the maximum value of magnetic flux density in the air gap, J_w – is the current density in the motor stator winding, B_s – is the average magnetic flux density in stator teeth.

The developed mathematical model allows the calculation following functional parameters of the designed motor: (a) motor efficiency (η), (b) total mass of constructional elements (m_t), and (c) temperature of motor winding in steady-state operation (ϑ_w). The adopted ranges of the design variables during the optimization process are presented in Table 2.

Table 2. Ranges of design variables.

Design variable	Unit	Upper	Lower
D_O	[mm]	75	180
B_δ	[T]	0.5	0.8
J_w	[A/mm2]	1.9	5.0
B_s	[T]	0.8	1.8

During the design of permanent magnet motors for electric vehicle applications, the efficiency and economic parameters (total mass of materials used in the motor construction) are very important [39].

Taking into account the above design assumptions, the authors proposed the following form of the multi-objective objective function for each whale:

$$\boldsymbol{f(D_o,\ B_\delta,\ J_w,\ B_s)}=\alpha\left(\frac{\eta}{\eta_0}\right)+\boldsymbol{\beta}\left(\frac{\boldsymbol{m_0}}{\boldsymbol{m_t}}\right) \quad (15)$$

in which: η_0 and m_0 are average reference values of efficiency and total mass of the constructional materials, respectively, α and β are the weighting coefficients.

Using the analytical model of the BLDC motor, a large number of simulation tests were performed, the values of the characteristic parameters of the WOA were obtained to obtain the best convergence and reliability, i.e. *b*, and *a* the type of change and parameters were determined. The *a* coefficient are non-linearly decreased in successive iterations of optimization process (see Fig. 5).

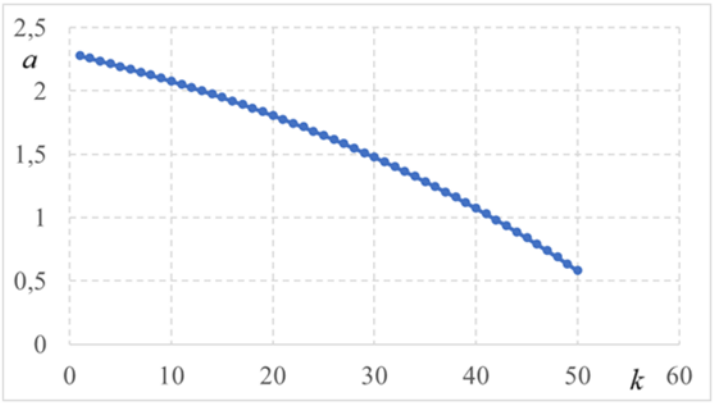

Figure 5. Changes in the coefficient *a* depending on the iteration number.

The optimization calculations were performed for the following parameters of the whale optimization algorithm: population size 60 whales, *b*=0.96, and *a* parameter non-linear decreasing from 2.28 to 0.58. The maximum number of iterations equal to 50 was adopted as a stop criterion. The optimization process was repeated 25 times for a random initial population.

The selection of equal values of the weighting coefficient caused the optimal motor with a small total mass, high winding temperature, and permanent magnets. The correct values of weighting factors were selected through many testing optimization processes for different values of weighting coefficients. Finally, the values of weighting coefficients were adopted: α=0.92 and β=0.08. The reference values of functional parameters were calculated as an average from five starting populations selected randomly. The following values of reference parameters were adopted: η_0=85.21 %, m_0=8.370 kg.

The statistical results for WOA are presented in Table 3.

Based on a series of 25 starts of the optimization procedure, the best optimal values of design variables for the designed BLDC motor were determined: D_O=120.10 mm, B_δ=0.758 T, J_w =2.01 A/mm^2, B_s =1.197 T. The optimal motor structure had the following functional parameters: η=89.21 %, m_t =5.758kg, and ϑ_w =80.755°C. It is worth mentioning that the WOA algorithm allows for the attainment of very good values of standard deviation for the values of the objective function, efficiency, and three design variables. Worst values of standard deviations were noted for the winding temperature, total mass, and the average magnetic flux density in stator teeth.

The comparison of the convergence curve for the best and worst optimization processes (for first 30-th iterations) in the analyzed series is shown in Figure 6.

Table 3. The statistical results for WOA.

Parameter	Best	Worst	AV	SD
D_O [mm]	120.10	121.01	120.59	1.84766E-10
B_δ [T]	0.758	0.698	0.745	0.016488644
J_w [A/mm^2]	2.01	2.01	2.01	2.84766E-9
B_s [T]	1.197	0.91	1.146	0.244489862
$f(D_o, B_\delta, J_w, B_s)$	1.047492149	1.0326341	1.046842042	0.000199867
η [%]	89.21	87.01	89.11	0.004170281
m_t [kg]	7.239	6.656	6.839	0.110242358
ϑ_w [°C]	90.755	95.115	91.860	1.859228939

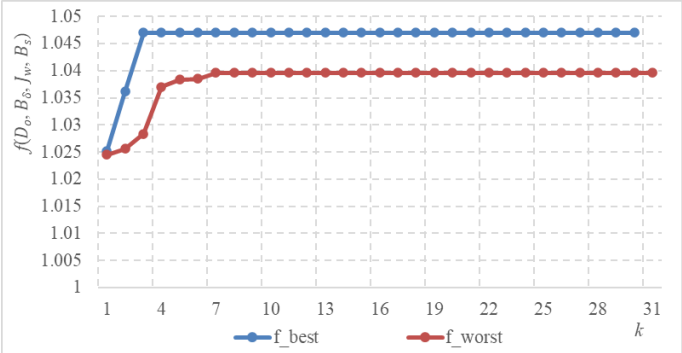

Figure 6. Comparison the convergence curves for best and worst optimization process.

From the comparison of convergence curves, it can be concluded that the convergence of the best optimization process is much better than the convergence of the worst optimization process. The worst optimization process is "stuck" at a local extremum point.

Next, optimization calculations were performed for the PSO optimization algorithm. The number of particles and the maximum number of iterations were adopted the same as for WOA optimization procedure. The following characteristic parameters of the PSO optimization procedure were: w=0.1, c_1=1.0 and c_2=1.1. The following values of reference parameters were adopted: η_0=85.21 % and m_0=8.370 kg. The statistical results from for PSO are presented in Table 4.

Table 4. The statistical results for PSO.

Parameter	Best	Worst	AV	SD
D_O [mm]	120.01	122.15	120.35	0.1581907
B_δ [T]	0.760	0.782	0.766	1.04741E-5
J_w [A/mm^2]	2.01	2.259	2.101	1.04766E-5
B_s [T]	1.414	1.194	1.402	0.0836925
$h(D_o, B_\delta, J_w, B_s)$	1.0380762	1.0369038	1.0379914	0.00252802
η [%]	89.22	87.63	88.99	0.00166176
m_t [kg]	7.239	6.773	6.939	0.4855378
ϑ_w [°C]	91.851	96.392	93.489	3.978364

Based on comparing the results for WOA and PSO algorithms, we noted that WAO allowed for determining a solution with a higher objective function value. The obtained values of design variables: D_o, J_w and B_δ are similar to the best solution, while differs B_s by value by about 18% between the two algorithms. The WOA algorithm is characterized by a smaller SD than the PSO algorithm.

Figure 7 presents a comparison of convergence for the best optimization process for PSO and WOA algorithms.

Next, the comparison for optimal values of design variables and selected functional parameters of the designed motor was compared (see Fig. 8).

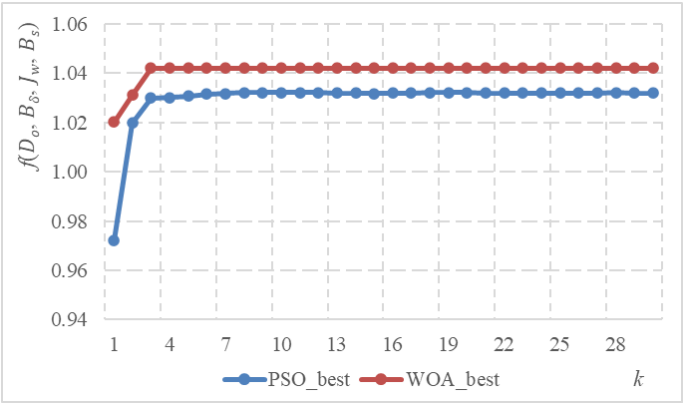

Figure 7. Comparison of the convergence curves for the best optimization process for WOA and PSO.

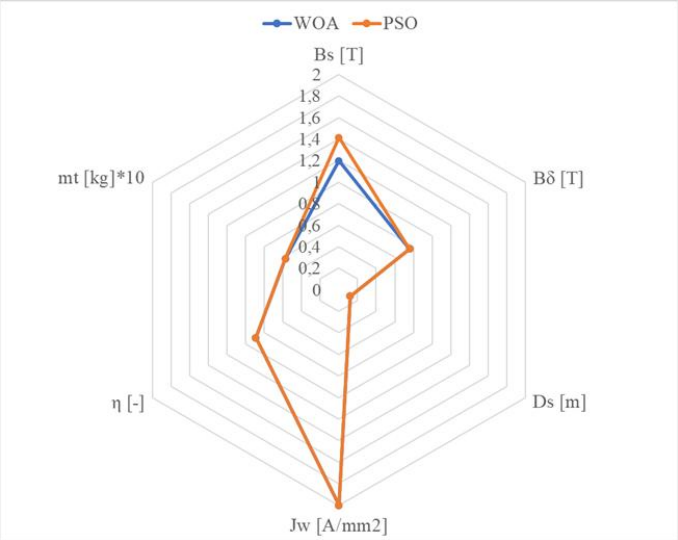

Figure 8. Comparison of optimal solutions for both analyzed optimization algorithms.

The optimal values of the design variables for both analyzed optimization algorithms are the same, with the exception of the stator tooth magnetic flux density. We also obtained similar values for the functional parameters of the optimized motor. Comparing the objective function values for both optimization algorithms, it can conclude that the WOA algorithm achieved a higher value of the multi-objective function. Moreover, analyzing the SD values, it can note that WOA is characterized by better reliability and efficiency. Better reliability and efficiency can be described as a greater probability of determining a global extremum point (variant of designed electromagnetic devices) for a single start of the optimization procedure.

In order to rate of the quality of the optimization calculation results, we also analyzed the skewness coefficient for the values of all objective functions for the analyzed series of optimization processes. For WAO, the value of skewness is 0.669, while for PSO, the skewness is -1.450.

In order to evaluate the algorithm's effectiveness and reliability in finding the optimal solution [39,40], the authors analyzed the results obtained during a series of 25 starts of the optimization procedure for a randomly selected initial population. Figure 9 and Figure 10 shows the frequency of occurrence of the final results of the optimization process for the WOA algorithm and PSO algorithm, respectively.

Based on the above histograms obtained from a series of 25 independent optimization processes, it can be observed that WOA achieved the best result for the maximized objective function. Furthermore, the best result was achieved 18 times out of 25 optimization runs. WOA is characterized by very good reliability in achieving the global maximum with a single run of the optimization procedure. In the case of PSO, the dispersion of the obtained results is larger, therefore, in order to obtain the optimal solution, the procedure should be run multiple times.

The above research have shown that the WOA algorithm is a very interesting tool for multi-objective optimization. Before starting the optimization computation, the WOA algorithm must be adapted to the optimization of the electromagnetic device by appropriately selecting the *a* and *b* coefficients.

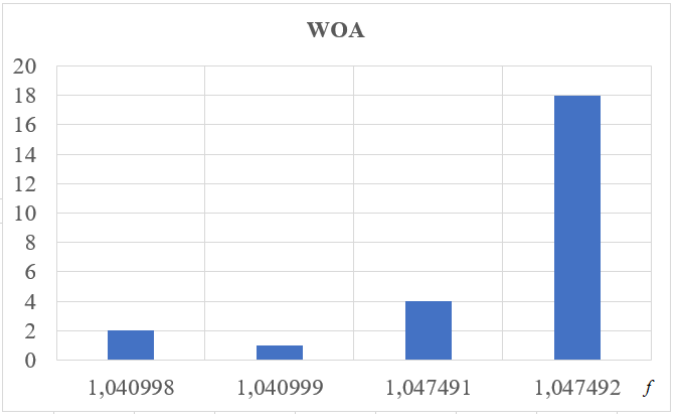

Fig. 9. Comparison of optimal solutions for WOA.

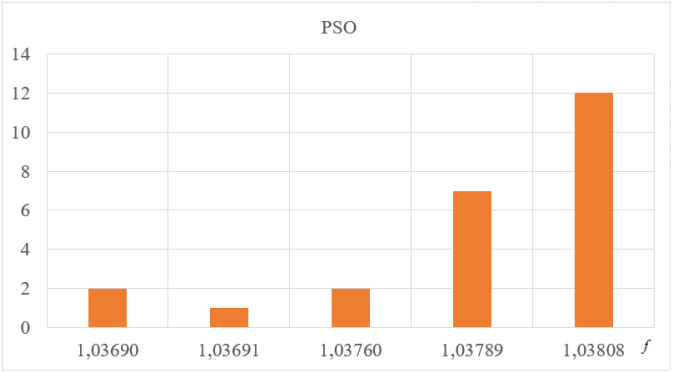

Fig. 10. Comparison of optimal solutions for PSO.

5.2. Constrained optimization

Then, the optimization problem was solved with imposed constraint concerning the selected functional parameter of the designed device. Very important designing parameters are also the mass of permanent magnets, the most expensive construction material, and the operating temperature of the machine [37]. Too high a temperature inside the machine can lead to thermal demagnetization of permanent magnets. Frequent start-ups of PM magnet motors can lead a large

over-currents, which can partially demagnetize the permanent magnets and irreversibly degrade the functional parameters of the designed motor and decrease reliability [38].

During solution a constrained optimization problem, an external penalty function method is applied. In elaborated approach a modified objective function *h* is constructed. The modified objective function is the sum of the primary objective function *f* and the penalty *p* representing the overstepping from the adopted constraints [11].

In the elaborated approach, the penalty was calculated as follows:

$$\boldsymbol{p}(\boldsymbol{D_o}, \boldsymbol{B_\delta}, \boldsymbol{J_w}, \boldsymbol{B_s}) = \kappa\Delta(\boldsymbol{D_o}, \boldsymbol{B_\delta}, \boldsymbol{J_w}, \boldsymbol{B_s}) \tag{16}$$

where: κ is the penalty coefficient, Δ is the non-linear constraint function representing the overstepping from the adopted permissible values.

The optimization problem took into account the constraint regarding the maximum winding temperature $\vartheta_w \leq \vartheta_z$. Then the nonlinear constraint function is defined as follows:

$$\Delta(\boldsymbol{D_o}, \boldsymbol{B_\delta}, \boldsymbol{J_w}, \boldsymbol{B_s}) = (\vartheta_w(\boldsymbol{D_o}, \boldsymbol{B_\delta}, \boldsymbol{J_w}, \boldsymbol{B_s}) - \vartheta_z)/\vartheta_z \tag{17}$$

where: ϑ_z is the imposed permissible winding temperature.

The elaborated approach assumes that the penalty coefficient will depend on the iteration number [21]. The value of the penalty will be updated in each iteration of the optimization algorithm. Considering the mathematical model of the adapted whale optimization algorithm and its good convergence, a series of optimization calculations was performed for the brushless DC motor model.

After performing many simulation computations, the authors proposed the following changes to the penalty coefficient:

$$\kappa = \sigma\frac{(k_{max}-k)^2}{k_{max}} \tag{18}$$

where: σ is the constant number, k_{max} is maximum number of iterations.

In the elaborated algorithm, the penalty coefficient changes in successive iterations of the optimization procedure. This approach ensures that the penalty changes smoothly, which ensures that individuals leave prohibited areas of the search space more quickly and ensures faster convergence of the optimization algorithm.

The authors adapted the external penalty function method to the whale optimization algorithm and the developed BLDC motor model. Many optimization test computations were performed for various linear and nonlinear functions describing the nature of the change in the penalty coefficient (κ). Figure 11 illustrates the changes of the penalty factor during optimization process.

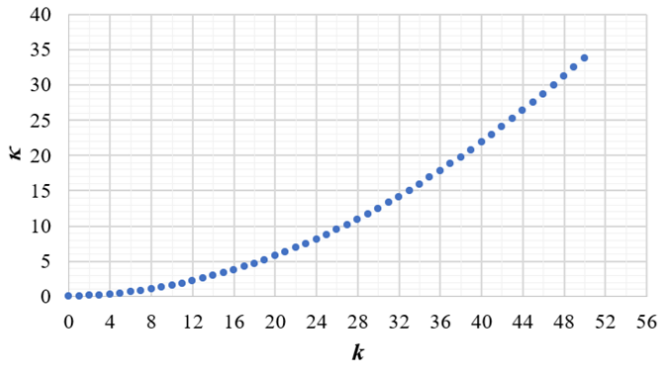

Figure 11. Changes to the penalty factor.

Finally the modified objective function has form:

$$\boldsymbol{h}(\boldsymbol{D_o}, \boldsymbol{B_\delta}, \boldsymbol{J_w}, \boldsymbol{B_s}) = \begin{cases} \boldsymbol{f}(\boldsymbol{D_o}, \boldsymbol{B_\delta}, \boldsymbol{J_w}, \boldsymbol{B_s}) & \text{for} \quad \vartheta_w \leq \vartheta_z \\ \boldsymbol{f}(\boldsymbol{D_o}, \boldsymbol{B_\delta}, \boldsymbol{J_w}, \boldsymbol{B_s}) - \boldsymbol{p}(\boldsymbol{D_o}, \boldsymbol{B_\delta}, \boldsymbol{J_w}, \boldsymbol{B_s}) & \text{for} \quad \vartheta_w > \vartheta_z \end{cases} \tag{19}$$

After performing many test computations to evaluate the efficiency and reliability of the optimization algorithm the value of σ=0.65 was assigned.

The reference values of functional parameters were calculated as an average from five starting populations selected randomly. The following values of reference parameters were adopted: η_0=85.21 %, m_0=8.370 kg. The imposed value of winding temperature ϑ_z=84°C was assigned. The optimization process was repeated 25 times to the random starting populations.

The statistical results from for WOA are presented in Table 5 and the statistical results from for PSO are presented in Table 6.

In the case of constrained optimization, the skewness coefficient was also analyzed. For the tested series of optimization processes, the skewness coefficients obtained for WOA and PSO were -1.610 and -2.115, respectively.

The analysis of the series of optimization calculations performed is presented in the above tables. The maximum value of the modified objective function was achieved using the whale

algorithm. Also, mean values of the modified objective function are higher for a series of optimization computations obtained for WOA. The smallest modified objective function value achieved using the whale method is greater than the corresponding value achieved using the PSO.

Table 5. The statistical results for constrained optimization and WOA.

Parameter	Best	Worst	AV	SD
D_O [mm]	107.39	144.95	120.93	10.03542
B_δ [T]	0.796	0.522	0.692	0.087924
J_w [A/mm^2]	1.908	1.903	1.986	0.068427
B_s [T]	0.969	0.801	1.162	0.285358
$h(D_o, B_\delta, J_w, B_s)$	1.073157	1.041009	1.063422	0.009106
η [%]	89.467	87.583	88.87	0.64557
m_t [kg]	5.575	5.990	5.681	0.27042
ϑ_w [°C]	84.093	83.24482	83.973	0.66902

Table 6. The statistical results for constrained optimization and PSO.

Parameter	Best	Worst	AV	SD
D_O [mm]	110.23	142.22	122.024	13.2136
B_δ [T]	0.768	0.616	0.693	0.07676
J_w [A/mm^2]	2.098	2.959	2.242	0.33312
B_s [T]	0.942	0.997	1.123	0.19539
$h(D_o, B_\delta, J_w, B_s)$	1.064061	1.000467	1.044692	0.01023
η [%]	88.685	85.72	87.91	1.393326
m_t [kg]	5.496	5.726	5.58	0.133874
ϑ_w [°C]	88.868	90.391	89.101	1.83646

Analysis of the obtained functional parameters for optimal solution showed that higher efficiency was achieved for the WOA algorithm, while lower mass was achieved for the PSO algorithm. Unfortunately, in the case of PSO, the imposed winding temperature has been exceeded. Based on the average winding temperature for a series of optimization calculations, it was observed to be very close to the imposed value of the ϑ_z. Therefore, it can be concluded that the penalty function adaptation was performed correctly. The standard deviation is approximately 0.66°C, which shows that despite the adaptation, the individual winding temperature values for each optimization process are different.

In the case of the PSO algorithm, it can be concluded that the procedure achieves a better mass than the WOA algorithm, but the optimal result does not meet the imposed constraint. After carefully analyzing the average winding temperature value from all optimization processes, it can be observed that the PSO algorithm has difficulty meeting the imposed constraint.

The PSO algorithm converges quickly and is characterized by a strong swarm effect consisting of the clustering of particles around leader position [4]. Therefore, in the case of this algorithm, the penalty must increase faster compared to the WOA algorithm, which, due to the sophisticated mathematical model, is characterized by resistance to getting "stuck" at the local extremum points and reliability in finding the global extremum when taking into account the constraints in the design process.

Figures 12 and 13 show the histograms of the optimization results (modified objective function and efficiency) for the WOA algorithm.

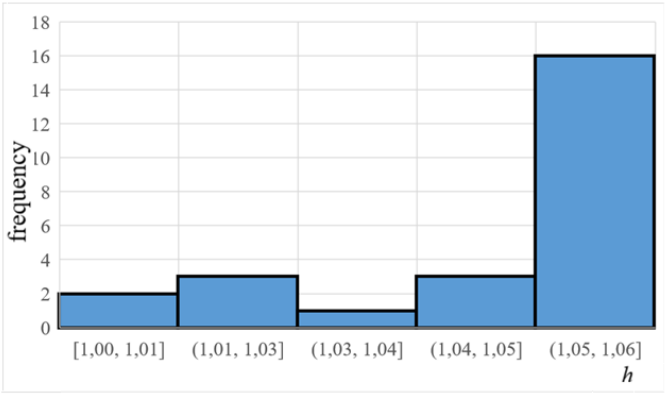

Fig. 12. Histogram of optimization results for modified objective function.

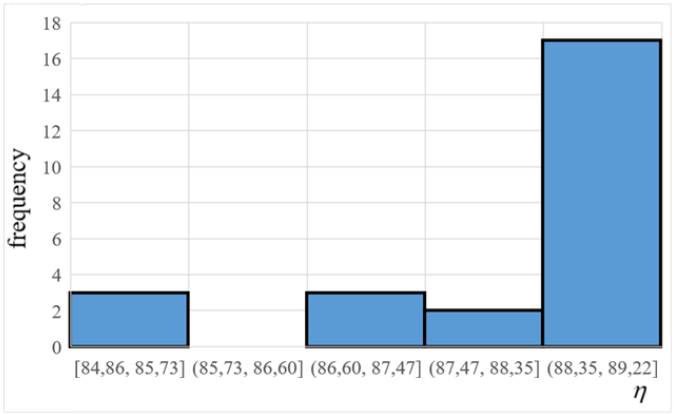

Fig. 13. Histogram of optimization results for efficiency.

Figures 14 and 15 presents the histograms of the optimization results (modified objective function and efficiency) for the PSO algorithm.

Based on the presented histograms for the WOA algorithm, we can note that both the highest range of the modified objective function and the highest efficiency for the analyzed series of optimization computation were obtained 16 times.

In the case of the PSO algorithm, the modified objective function values are obtained only 9 times, which is significantly less frequent than for the whale algorithm. Also for the second

tested algorithm, lower efficiency of the designed BLDC motor is usually obtained.

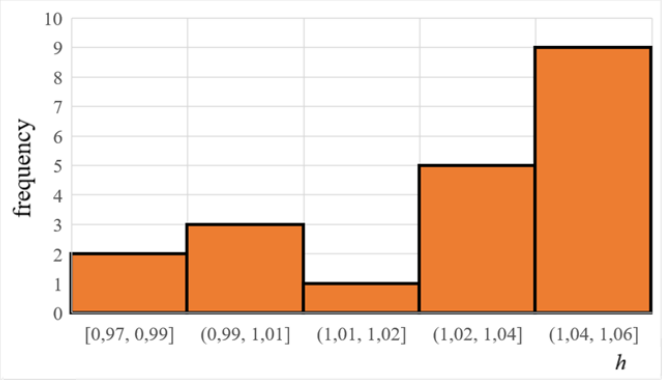

Fig. 14. Histogram of optimization results for modified objective function and PSO.

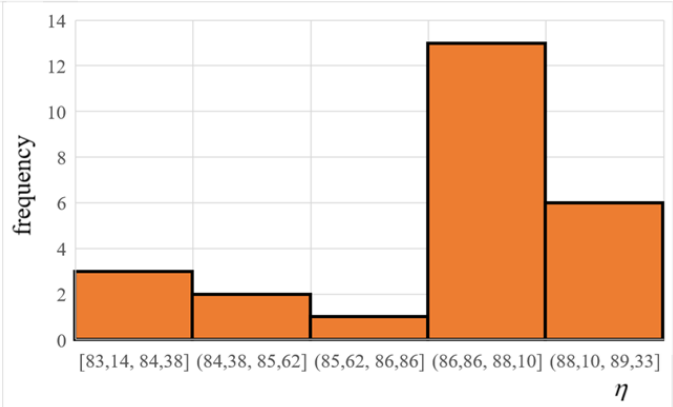

Fig. 15. Histogram of optimization results for efficiency and PSO.

The authors compared the total calculation time of the single optimization process for a series of 25 runs of optimization software for both algorithms. As previously established, both compared optimization procedures execute the same number of call functions. The WOA algorithm executes more operations to determine new whale positions in each iteration. Additionally, in each iteration, it is necessary to determine the value of a coefficient (Fig. 5) and the κ coefficient (Eq. 18). Based on the analysis of the total calculation time of the optimization procedure for WOA, we obtained a time increase of 1.36% in comparison to PSO for the analytical model. It should be noted that for the field model, the time difference will be negligible.

6. Finite element analysis verification

For the optimal structure of BLDC obtained as a result of optimization using the WOA algorithm, a mathematical model was developed using two-dimensional finite element analysis (FEA). FEA verification was made in Ansys Maxwell environment.

In permanent magnet machines, especially in BLDC motors, the electromagnetic field is excited by two sources: the permanent magnets and the windings distributed in the stator. The main equations describing distribution of the electromagnetic field in BLDC motors have a form:

$$\mathrm{curl}\left(\frac{1}{\mu}\mathrm{curl}\mathbf{A}\right) = \boldsymbol{J_w} + \boldsymbol{J_{PM}} \tag{20}$$

$$\boldsymbol{J_w} = \boldsymbol{\gamma}\left(\mathrm{grad}\boldsymbol{V_e} - \frac{\boldsymbol{\partial A}}{\boldsymbol{\partial t}}\right) \tag{21}$$

where: μ is the magnetic permeability, **A** is the magnetic vector potential, $\mathbf{J}_w$ is vector of current density winding, $\mathbf{J}_{PM}$ is the vector of magnetizing current density in the permanent magnets region $\mathbf{J_{PM}} = \mathrm{curl}\,\mathbf{M}$ [43], γ is the electric conductivity, V_e is the scalar electrical potential.

The electromagnetic devices are supplied by voltage sources. Due to the non-linearity of the ferromagnetic core and inducted back-electromotive forces in phase winding, the waveforms of current in the separated stator phases of the BLDC motor are not known in advance. The waveforms of the phase currents are necessary to solve equation (21). To determine the current waveforms it is necessary to take into consideration the Kirchhoff equations for electric circuits:

$$\frac{\boldsymbol{d\Psi}}{\boldsymbol{dt}} + \boldsymbol{Ri} = \boldsymbol{u} \tag{22}$$

where: **u** is vector of phases supply voltages, **Ψ** is the matrix of flux linkage, ***R*** is the diagonal matrix of winding resistances, **i** is the vector of BLDC phase currents.

During a change in loading torque, the transient operation state causes a change in rotational speed. Therefore, it is necessary to take into account the mechanical equation of rotary machines:

$$\boldsymbol{J_i}\frac{\boldsymbol{d\omega}}{\boldsymbol{dt}} = \boldsymbol{T} - \boldsymbol{T_{lo}} - \boldsymbol{B\omega} \tag{23}$$

where J_i is the moment of inertia, ω is the angular velocity, T is the output torque, T_{lo} is the loading torque, B is the friction coefficient.

The BLDC motor with main dimensions obtained using the WOA optimization algorithm was modelled in the Ansoft Maxwell. The 2D FEA model is developed. Next, the efficiency for different loading torques was analyzed. The results of the simulation computation are presented in the Figure 16.

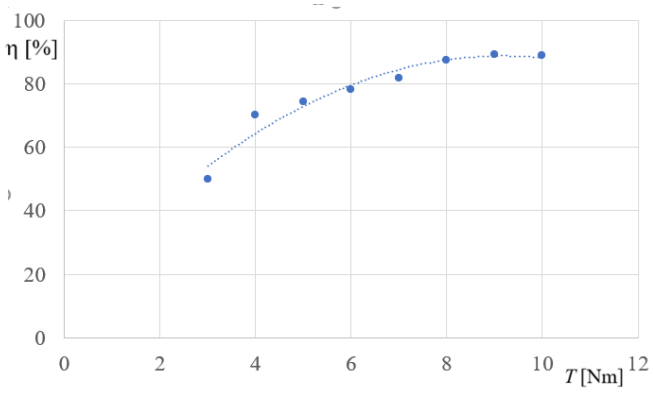

Figure 16. The characteristic of the efficiency versus the loading torque.

For the rated loading torque, the optimal motor structure obtained efficiency equal 88.4%. The highest efficiency was achieved for a load of 0.9 T_N and was equal 88.9%. FEA calculations confirmed a good convergence between the BLDC motor analytical model and the FEA model.

7. Conclusions

This paper presents an adaptation of the external penalty function method to the whale optimization algorithm. A constrained optimization problem for a brushless DC motor was analyzed. The WOA algorithm was adapted by correctly selecting characteristic coefficients (a and b) for the optimization algorithm to optimize electromagnetic devices. In the second stage, the penalty function was adapted to solve the constrained optimization problem. This adaptation involved selecting the nature of the penalty factors changes.

The paper proposes an approach in which the penalty coefficient and the penalty increase smoothly in each iteration of the optimization algorithm; such adaptation increases the efficiency and reliability of the optimization algorithm. The above analysis of statistical measures presents a better performance and reliability of the WOA.

Analysis of the optimization results' histograms (Fig. 12 and Fig. 14) showed that the most effective approach for the considered task is the whale algorithm. Thus elaborated adaptation, the software user has the highest probability of obtaining the optimal result in a single run of the optimization algorithm.

The optimization calculations performed showed that after selecting an optimization algorithm, it is necessary to proper select the characteristic coefficients of the optimization algorithm for the solved optimization problem (electromagnetic devices). After selecting the characteristic coefficients for the selected optimization algorithm, it is necessary to made adaptation the penalty function method by selecting the appropriate type of changing penalty factor.

The developed algorithm and optimization software are universal. Software allows the connection of the master optimization module with different permanent magnet motor models. Analytical models, lumped parameter models and FEM models can be joined with optimization module. This is because the optimization module sends to the model only information about the current value of the decision variables vector. The presented algorithm can be applied to optimal design permanent magnet synchronous motors, synchronous reluctance motors (SynRM), line-start permanent magnets motors (LSPMSM) and also permanent magnet assisted (SynRM). It should be underlined that after changing the structure of the optimized device or mathematical model, the adaptation process by proper selecting characteristic coefficients and penalty coefficient should be executed.

In future research, we plan to investigated method of adaptation the WOA to multi-objective optimization and constrained optimization. The optimization procedure will be coupled with a 2D FEM model of the BLDC motor.

References

1. Faramarzi Palangar M, Soong W, Bianchi N, Wang R J. Design a Optimization Techniques in Performance Improvement of Line-Start Permanent Magnet Synchronous Motors: A Review. IEEE Transactions on Magnetics 2021; 57(9), https://doi.org/910.1109/TMAG.2021.3098392.
2. Lei G, Zhu J, Guo Y, Liu C, Ma B. A Review of Design Optimization Methods for Electrical Machines. Energies 2017; 10 (1962): 1–31, https://doi.org/10.3390/en10121962.
3. Arya A K, Jain R, Yadav S, Bisht S, Gautam S. Recent trends in gas pipeline optimization. Materials Today: Proceedings 2022; 57(4): 1455–1461, https://doi.org/10.1016/j.matpr.2021.11.232.
4. Liu Q, Sun R, Bu X, Hanajima N, Ding W. Optimal Trajectory Planning Method for Handling Robots Based on Multi-objective Particle

Swarm Optimization Guided by Evolutionary Information. Eksploatacja i Niezawodnosc – Maintenance and Reliability 2025: 27(4): 1–20, http://doi.org/10.17531/ein/202990.

5. Muhammad N, Khan F, Ullah B, Alghamdi B, Performance analysis and design optimization of asymmetric interior permanent magnet synchronous machine for electric vehicles applications. IET Electrical Power Applications 2024; 18(4): 425–435, https://doi.org/10.1049/elp2.12402.
6. Cvetkovski G V, Petkovska L. Selected Nature-Inspired Algorithms in Function of PM Synchronous Motor Cogging Torque Minimisation. Power Electronics and Drives 2021; 6(41): 1–14, https://doi.org/10.2478/pead-2021-0012.
7. Knypiński L. Constrained optimization of line-start PM motor based on the gray wolf optimizer. Eksploatacja i Niezawodność – Maintenance and Reliability 2021; 23(1): 1–10, https://doi.org/10.17531/ein.2021.1.1.
8. Knypiński Ł. A novel hybrid cuckoo search algorithm for optimization of a line-start PM synchronous motor. Bulletin of the Polish Academy of Sciences Technical Sciences 2023; 17(1): 1–8, https://doi.org/10.24425/bpasts.2023.144586.
9. Selvarajan S. A comprehensive study on modern optimization techniques for engineering applications. Artificial Intelligence Review 2024; 57: 1–52, https://doi.org/10.1007/s10462-024-10829-9.
10. Rajwar K, Deep K, Das S. An exhaustive review of the metaheuristic algorithms for search and optimization: taxonomy, applications, and open challenges. Artificial Intelligence Review 2023; 56: 13187–13257, https://doi.org/10.1007/s10462-023-10470-y.
11. Muñoz M A, Kirley M, Halgamuge S K. The Algorithm Selection Problem on the Continuous Optimization Domain. Computational Intelligence in Intelligent Data Analysis 2013; 445: 75–89, https://doi.org/10.1007/978-3-642-32378-2_6.
12. Asadianfam S, Emami H. An adaptive seasons optimization algorithm for global optimization, The Journal of Supercomputing 2025; 81 (1048), https://doi.org/10.1007/s11227-025-07511-4.
13. Pandya S, Jangir P, Mahdal M, Kalita K, Singh Chohan J, Abualigah L. Optimizing brushless direct current motor design: An application of the multi-objective generalized normal distribution optimization. Heliyon 2024; 10(e26369): 1–15, https://doi.org/10.1016/j.heliyon.2024.e26369.
14. Xue Z, Li Q, Liu P, Zhu W. Optimization of PM Slotless Brushless DC Motors Considering Magnetic Saturation and Temperature Limitation. Energies 2024; 17(2921): 1–22, https://doi.org/10.3390/en17122921.
15. Hyunjae L, Okunki L. Optimization of Brushless DC Motor Controllers for Energy-Efficient Motion Control Systems. National Journal of Electric Drives and Control System 2025; 1(2): 1–8, https://doi.org//10.17051/NJEDCS/01.02.01.
16. Aseer Khan M, Baig D, Ali H, Albogamy F, Optimized System Identification (SI) of Brushless DC (BLDC) motor using Data-Driven. Modeling Methods, Scientific Reports 2025; 15(8497): 1–20, https://doi.org/10.1038/s41598-025-93444-0.
17. Paplicki P, Palka R. Effects of additional magnets and iron components in the rotor on flux control of a hybrid-excited synchronous machine. Archives of Electrical Engineering 2025; 74(3): 603-616, https://doi.org/10.24425/aee.2025.154986.
18. Tomar V, Bansal M, Singh P. Metaheuristic Algorithms for Optimization: A Brief Review. Engineering Proceedings 2023; 58(238), https://doi.org/10.3390/engproc20230592.
19. Mirjalili S, Lewis A. The Whale Optimization Algorithm. Advances in Engineering Software 2016; 95: 51–67, https://doi.org/10.1016/j.advengsoft.2016.01.008.
20. Li C, Yao Y, Jiang M, Zhang X, Song L, Zhang Y, Zhao B, Liu J, Yu Z, Du X, Ruan S. Evolving the Whale Optimization Algorithm: The Development and Analysis of MISWOA. Biomimetics 2024; 9(10): 1–28, https://doi.org/10.3390/biomimetics9100639.
21. Wang J, Wang Y. An Efficient Improved Whale Optimization Algorithm for Optimization Tasks. Engineering Letters 2024; 32(2): 392–411, https://doi.org/10.1007/s44163-026-00854-8.
22. Gaoa B, Yangb H, Lin H, Wanga Z, Zhangd W, Li L. A Hybrid Improved Whale Optimization Algorithm with Support Vector Machine for Short-Term Photovoltaic Power Prediction. Applied Artificial Intelligence 2022: 36(1): 1–33, https://doi.org/10.1080/08839514.2021.2014187.
23. Xu T, Chen C. DBO-AWOA: An Adaptive Whale Optimization Algorithm for Global Optimization and UAV 3D Path Planning. Sensors 2025; 25(2336): 1–22, https://doi.org/10.3390/s25072336.
24. Guo W, Li S, Dai F, Wang F, Zhang W. A two-stage large-scale multi-objective optimization approach incorporating adaptive entropy and enhanced competitive swarm optimizer. Expert Systems with Applications 2025; 278 (127374),

https://doi.org/10.1016/j.eswa.2025.127374.
25. Hasanien H M. Whale optimisation algorithm for automatic generation control of interconnected modern power systems including renewable energy sources. IET Generation, Transmission & Distribution 2017; 12(3): 607-614, https://doi.org/10.1049/iet-gtd.2017.100.
26. Simmonds M P. Into the brains of whales. Applied Animal Behaviour Science 2006; 100 (1–2): 103–116, https://doi.org/10.1016/j.applanim.2006.04.015.
27. Hain J, Carter G, Kraus S, Mayo C, Winni H. Feeding behavior of the humpback whale, Megaptera novaeangliae, in the western North Atlantic. Fishery Bulletin 1982; 80(2).
28. Wiley D, Ware C, Bocconcelli A, Cholewiak D, Friedlaender A, Thompson M, Weinrich M. Underwater components of humpback whale bubble-net feeding behaviour. Behaviour 2011; 148(5–6): 575–602, https://doi.org/10.1163/000579511X570893.
29. Mirjalili S. Handbook of Whale Optimization Algorithm: Variants, Hybrids, Improvements, and Applications. London San Diego, CA: Academic Press, Elsevier, 2024.
30. Reddy K, Saha A K. A modified Whale Optimization Algorithm for exploitation capability and stability enhancement. Heliyon 2022; 8(10): e11027, https://doi.org/10.1016/j.heliyon.2022.e11027.
31. Czerniak J M, Ewald D, Paprzycki M, Fidanova S, Ganzha M. A New Artificial Duroc Pigs Optimization Method Used for the Optimization of Functions. Electronics 2024; 13(70): 1–19, https://doi.org/10.3390/electronics13071372.
32. Deng W, Ma X, Qiao W. A Hybrid Intelligent Optimization Algorithm Based on a Learning Strategy. Mathematics 2024; 12(16), 1–17, https://doi.org/10.3390/math12162570.
33. Amin R, El-Taweel G, Ali A F, Tahoun M. Hybrid Chaotic Zebra Optimization Algorithm and Long Short-Term Memory for Cyber Threats Detection. IEEE Access 2024; 12, 93235–93260, https://doi.org/10.1109/ACCESS.2024.3397303.
34. Terzić M, Mihić D. Switched Reluctance Motor Design for a Mid-Drive E-Bike Application. Machines 2022; 10(8): 1–26, https://doi.org/10.3390/machines10080642.
35. Cheng Y, Lyu X, Mao S. Optimization design of brushless DC motor based on improved JAYA algorithm. Scientific Reports 2024; 14(5427): 1–19, https://doi.org/10.1038/s41598-024-54582-z.
36. Brisset S, Brochet P. Analytical model for the optimal design of a brushless DC wheel motor. Compel 2005; 24(3): 829–848, https://doi.org/20.1108/03321640510612952.
37. Knypiński Ł, Reddy A V, Venkateswararao B, Devarapalli R. Optimal design of brushless DC motor for electromobility propulsion applications using Taguchi method. Journal of Electrical Engineering 2023; 74(2): 116–121, https://doi.org/10.2478/jee-2023-0015.
38. Vukotić M, Lutovski S, Šutar N, Miljavec D, Čorović S. Thermal Effects in the End-Winding Region of Electrical Machines. Energies 2023; 16(2), 1–22, https://doi.org/10.3390/en16020930.
39. Contò C, Bianchi N. Design of electric motor for e-bike application. 2023 IEEE International Electric Machines & Drives Conference (IEMDC), 15-18 May 2023, San Francisco, CA, USA ,https://doi.org/10.1109/IEMDC55163.2023.10238875.
40. Barański M, Demenko A, Szeląg W, Łyskawiński W. Experimental verification of temperature effects on functional parameters in a line start permanent magnet synchronous motor. IET Science, Measurement & Technology 2024; 18(9): 491–498, https://doi.org/10.1049/smt2.12206.
41. Ampellio E, Gjorgiev B, Sansavini G. Multi-level informed optimization via decomposed Kriging for large design problems under uncertainty. Reliability Engineering & System Safety 2026; 70(112060), https://doi.org/10.1016/j.ress.2025.112060.
42. Haris H, Nam H. Path Planning Optimization of Smart Vehicle With Fast Converging Distance-Dependent PSO Algorithm. IEEE Open Journal of Intelligent Transportation Systems 2024; 5: 726–739, https://doi.org/10.1109/OJITS.2024.3486155.
43. Moll D, D'Angelo L, De Gersem H, Boattini F, Bottura L, Gast M. A Dynamic Energy-Based Hysteresis Model for Pulsed-Operated Fast-Ramping Magnets. IEEE Transactions on Magnetics 2025; doi: https://doi.org/10.1109/TMAG.2025.3639643.